SS Multidisciplinary Research Journal Vol. 2, No. 1 (2025)

Received:30 July, 2025 Revised: 30 AUGUST, 2025 Accepted: 6, November 2025

Seasonal Variation of Solar Wind–Geomagnetic Coupling: A Correlation Heatmap Approach

Prajwal Bhandari[1], Kiran Bagale[2], Bidur Nepal[3]
Assistant Professor Madan Bhandari Memorial College
Assistant Professor Madan Bhandari Memorial College
Assistant Professor Patan Multiple Campus

DOI: https://doi.org/10.3126/ssmrj.v2i1.86642

Abstract

Solar wind–magnetosphere interaction during geomagnetic storm periods is visually demonstrated by the graphics that show the statistical and temporal links between important solar wind parameters and geomagnetic indices. Significant variations in variables including the interplanetary magnetic field (BZ), solar wind proton density, plasma speed, flow pressure, and geomagnetic indices (Dst and AE) are seen in the continuous time series charts. The dynamic solar wind conditions that cause magnetospheric disruptions are reflected in these fluctuations.

The degree and direction of inter-parameter dependencies are further demonstrated by the correlation heatmaps for January and July, which show significant negative correlations between BZ and AE or Dst indices and strong positive correlations between proton density and flow pressure. These correlations confirm that southbound BZ components increase geomagnetic activity by encouraging energy transfer and magnetic reconnection into Earth's magnetosphere. In line with other findings in space weather research, the statistics generally support the notion that storm generation and geomagnetic variations are dominated by the interplanetary magnetic field BZ.

Keywords: *Solar wind, Geomagnetic storms, Correlation analysis, Interplanetary magnetic field, Magnetospheric coupling.*

Introduction

Solar wind is a stream of charged particles, mostly electrons and protons, which are energized and flow outward from the Sun through the solar system at a speed of around 400 km/s. It is composed of plasma and has a temperature of one million degrees Celsius (Parker, 1958). The sun releases about 100 tons of solar wind every day. It has a lot of electrical and kinetic energy. The planet gets heated as a result of some of these energies directly entering the magnetosphere. These energies also disrupt geomagnetic activity as they enter the magnetosphere, which eventually leads to geomagnetic storms, sub-storms, and auroras (Gonzalez W. D., 1999). When the solar wind's magnetic field interacts with the earth's magnetic field after entering the magnetosphere, it produces a temporary disturbance. (Dungey, 1961)

When the solar wind pressure goes up, the earth's magnetosphere becomes initially compressed. A certain amount of energy is increased during the interaction between the earth's magnetic field and the solar wind magnetic field. This increased energy eventually raises the magnetosphere's plasma level and increases the movement of electric current in the magnetosphere and ionosphere (Dungey, 1961; Gonzalez W. a.-A., What is a geomagnetic storm?, 1994). Based on the Dst measurement, the geomagnetic storms are divided into four groups: weak/small (-30nT to -50nT); moderate (-50nT to -100nT); intense (-100nT to -250nT); and very intense (-250nT and above) (Gilles-Gonzalez, 1994).

All of those occurrences are caused by a chaotic dynamo at the sun's surface, which produces minor magnetic field fluctuations, and a helical dynamo around the sun's mass center, which produces a high magnetic field (Kivelson, 1995). Space weather refers to the cumulative effects of solar variations within the sun's gravitational field, and solar variation is the total of all these changes. The periods that fall under solar activity are known as solar minima and solar maxima. Solar minima is the time in the sun's 11-year cycle when solar activity is at its lowest. During this time, sunspot and solar flare activity decreases and occasionally doesn't happen for several days. Since the minimum is characterized by a smoothed average over a 12-month period of sunspot activity, solar minima can only be identified six months after they actually occur. Solar maxima are the typical times throughout the sun's 11-year solar cycle when solar activity is at its highest. The earth's global climate is directly impacted by the enormous number of sunspots that arise at this time and the sun's irradiance output, which increases by around 0.07%. (Burlaga, 1995; Harvey, 2000). Geomagnetic indices are used for determining all short-term geomagnetic disturbances. It was discovered that there are large variations in the magnetic field measured close to the earth's surface. The solar wind's interaction with the earth's magnetosphere and the magnetosphere's interaction with the ionosphere are the primary causes of fluctuations in the geomagnetic field (Dungey, 1961; Gonzalez W. a.-A., What is a geomagnetic storm?, 1994). The Dst index along with AE index are the primary metrics used to gauge changes in the strength of the magnetic field of the planet (Sugiura, 1964; Rostoker, Geomagnetic indices, 1972). The global magnetic storm level is tracked using a temporary disturbance (Dst) index. It is built by averaging H from equatorial magneto grams and midlatitude magneto grams worldwide. The Dst index is negative, indicating the presence of a magnetic storm. This is caused by the storm time ring current, which circles the planet on the equatorial plane from east to west. The severity of the magnetic storm increases with a greater negative value of Dst. The sun's activity determines the ranges of Dst values. The observed Dst values are about between +100 nT and -600 nT. The compression of magnetosphere brought on by an increase in solar wind pressure is the cause of the Dst's positive value. AE measures the global auroral zone magnetic activity caused by increased ionospheric current. (Rostoker, Geomagnetic indices, 1972; Burgess, 1995). The electric current that rounds the ionosphere's zones D and E regions is known as an electro jet. It is built using oneminute datasets of H-components from global auroral zone observatories. Plotting the generated values as a function of universal time (UT) is thus done. The terms “AU" and "AL" refer to the amplitude of the upper and lower envelopes, respectively. The highest disturbance caused by the eastward electro jet current in the afternoon sector is represented by the amplitude of AU, while the maximum disturbance caused by the westward electro jet current in the morning and midnight sectors is represented by the amplitude of AL. The AE index is calculated as the difference between AU and AL, while the AO index is calculated as (AU + AL)/2. Generally speaking, AU, AL, AE, and AO are denoted by the phrase "AE." Heatmap is used to find the correlation between the parameters.

Data Set and methodology

We applied an online data source from OMNI (Operating Mission as Nodes on the Internet web system), an international space center (https://omniweb.gsfc.nasa.gov/ow.html). For a very long time, the OMNI system has been employing several GPS and satellite stations both on Earth and in space to perform its study. For the benefit of those like us, the results of their observations and research are maintained on the website. We look at two distinct geomagnetic storms and examine how solar wind characteristics change during geomagnetic storms at a certain moment. We used heatmap to find the correlation between wind parameters.

Result and discussion

Case1: Geomagnetic Strom in 2025 January 1 to 2025 January 30 (720 Hours)

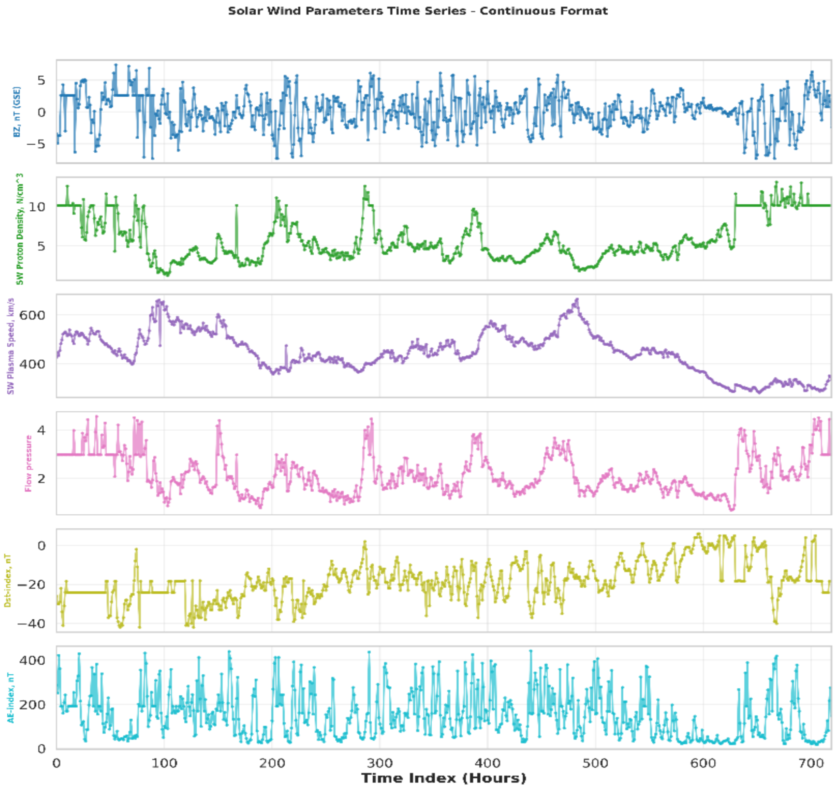

The temporal evolution of important solar wind and geomagnetic parameters during the course of the investigation is shown in Figure 1 in a continuous hourly manner. The interplanetary magnetic field (IMF) Bz component (in GSE coordinates) is displayed in the top panel. It frequently fluctuates between northward and southward orientations, with notable southward excursions (negative Bz) usually linked to increased geomagnetic activity and possible times of magnetic reconnection at the dayside magnetopause. The solar wind proton density, which fluctuates greatly during the interval, is shown in the second panel. It reveals several high-density structures that are probably connected to interplanetary shocks or stream interaction zones. The solar wind plasma speed in the third panel steadily increases over a number of intervals, indicating the passage of high-speed solar wind streams that originate from coronal holes. The impact of density improvements on magnetospheric compression is confirmed by the dynamic pressure (fourth panel), which varies similarly to the density. The AE index (bottom panel) displays multiple spikes linked to substorm activity, reflecting variations in auroral electrojet strength driven by solar wind–magnetosphere coupling, while the Dst index (fifth panel) displays several negative excursions corresponding to geomagnetic storm events, indicating enhanced ring current intensity during those times. Overall, the time series analysis shows that periods of high solar wind speed and negative IMF Bz are associated with increased geomagnetic disturbances, as shown by elevated AE indices and depressed Dst, underscoring the close relationship between solar wind conditions and the level of geomagnetic activity seen at Earth on 2025 1st January to 30th January.

Case 2: Geomagnetic Strom occurred in 2025 July 1 to 2025 July 30 (700 hours)

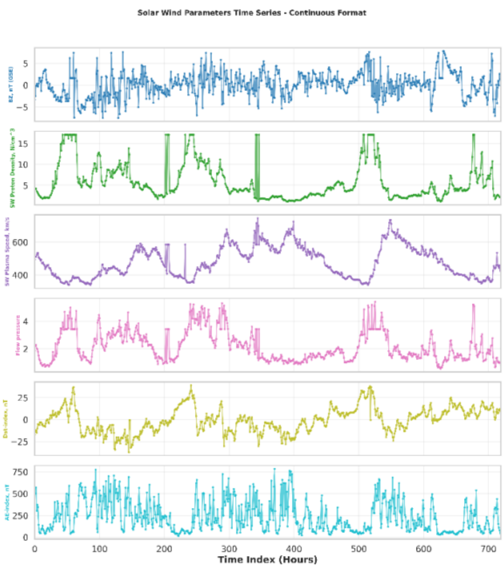

The continuous hourly change of important solar wind and geomagnetic parameters is shown in Figure 1, emphasizing their dynamic nature throughout the observation period. Geomagnetic activity levels are influenced by alternating northward and southbound magnetic orientations, as shown by the interplanetary magnetic field (IMF) Bz component (top panel), which varies between positive and negative values. The solar wind proton density (second panel) exhibits many abrupt rises, indicating the existence of high-density plasma areas that are probably connected to interplanetary shocks or solar wind compression. High-speed solar wind streams emerging from coronal holes are characterized by periodic boosts surpassing 600

Figure 2: Geomagnetic Storms on 1st July to 30th July 2025.

km/s in the solar wind plasma speed (third panel). The dynamic pressure's involvement in modifying magnetospheric compression is demonstrated by its variability, which is consistent with density changes (fourth panel). Increased ring current activity is shown by many negative excursions in the Dst index (fifth panel), which correlate to geomagnetic storm episodes. Frequent spikes in the AE index (bottom panel) indicate increased auroral electrojet activity and substorm events. Overall, the time series analysis confirms the solar wind's dominant control over magnetospheric disturbances by showing a substantial link between negative IMF Bz, increased solar wind speed, and increased geomagnetic activity.

3.2Heatmaps

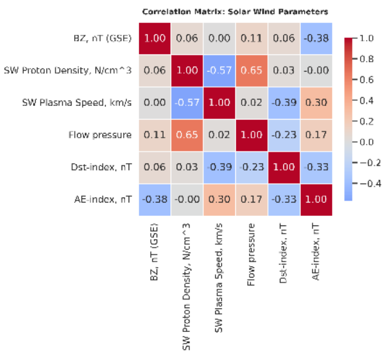

The correlations between several solar wind characteristics are shown in the January correlation matrix (first figure). The figure shows a significant positive association (r = 0.65) between solar wind proton density and flow pressure, indicating that higher proton density usually correlates with higher flow pressure. On the other hand, there is a negative connection (r = -0.57) between the solar wind plasma speed and proton density, suggesting that dense

Figure 3: Heatmap on 1st January to 30th January 2025

solar winds are often slower. Furthermore, the BZ component has a modest association with the majority of parameters but a somewhat negative correlation (r = -0.38) with the AE-index, indicating that geomagnetic activity is often enhanced by southward magnetic fields.

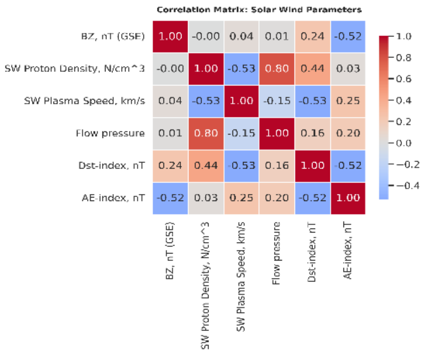

An increased solar wind interaction under mid-year circumstances is shown by the July correlation matrix (second figure), which displays a greater coupling among parameters, especially between flow pressure and solar wind proton density (r = 0.80). Additionally, the Dst-index has a positive association with BZ (r = 0.24) and proton density (r = 0.44), suggesting that fluctuations in these parameters during July are more closely associated with geomagnetic storms. Additionally, AE-index

Figure 4: Heatmap on 1st July to 30th July 2025.

shows a high negative connection with both BZ (r = -0.52) and Dst-index (r = -0.52), suggesting that storm-time depressions in the geomagnetic field and southward IMF are associated with increased auroral activity.

Conclusion

Significant conclusions into cosmic-terrestrial interactions may be gained by analyzing solar wind characteristics using correlation heatmaps and time series visualization. Significant temporal variability in all parameters is shown by the continuous time series charts, which show clear variations in BZ, proton density, plasma speed, and flow pressure with time. These dynamic shifts show how solar wind behavior is intricate and interconnected, with changes in one parameter frequently having an impact on others. The geomagnetic reaction to solar wind disturbances is shown in the trends in the Dst and AE indices, which show how changes in interplanetary magnetic fields and plasma conditions influence geomagnetic activity on various time periods.

The correlation heatmaps for January and July further illustrate the seasonal shift in inter-parameter interactions. Strong positive correlations between flow pressure and proton density and negative correlations between plasma speed and density validate consistent physical interactions inside the solar wind. Furthermore, there is a substantial negative correlation between BZ and the AE and Dst indices, suggesting a relationship between southbound IMF and geomagnetic storm strength. Overall, the findings highlight the significance of both temporal patterns and parameter correlations in understanding space weather dynamics, providing helpful data for predictive modeling and geomagnetic activity prediction.

References

Burlaga, L. F. (1995). *burlaga1995interplanetary.* Oxford University Press.

Dungey, J. W. (1961). Interplanetary magnetic field and the auroral zones. p. 47.

Gilles-Gonzalez, M. A. (1994). Heme-based sensors, exemplified by the kinase FixL, are a new class of heme protein with distinctive ligand binding and autoxidation. p. 8067.

Gonzalez, W. a.-A. (1994). What is a geomagnetic storm? *Journal of Geophysical Research: Space Physics*, 5771 - - 5792.

Gonzalez, W. a.-A. (1994). What is a geomagnetic storm? *99*, 5771--5792.

Gonzalez, W. D. (1999). Interplanetary origin of geomagnetic storms. pp. 529--562.

Harvey, D. (2000). *Spaces of hope* (Vol. 7). Univ of California Press.

Kivelson, M. a. (1995). In MG Kivelson \& CT Russell. *Introduction to space physics*, 1995.

Parker, E. N. (1958). Dynamics of the interplanetary gas magnetic fields. *Astrophysical Journal*, p. 664.

Rostoker, G. (1972). Geomagnetic indices. *Reviews of Geophysics*, 935 - - 950.

Rostoker, G. (1972). Geomagnetic indices. *10*, 935--950.

Sugiura, M. a. (1964). Oscillation of the geomagnetic field lines and associated magnetic perturbations at conjugate points. *Journal of Geophysical Research*, *69*, 12 - - 1216.